[1-9-NαC]-crourorb A1 isolated from Croton urucurana latex induces G2/M cell cycle arrest and apoptosis in human hepatocarcinoma cells

Priscila De Matos Cândido-Bacani, Frédéric Ezan, Patrícia De Oliveira Figueiredo, Maria de Fátima Cepa Matos, Fernanda Rodrigues Garcez, Walmir Silva Garcez, Georges Baffet

[1–9-NαC]-crourorb A1 isolated from *Croton urucurana* latex induces G2/M cell cycle arrest and apoptosis in human hepatocarcinoma cells

Priscila de Matos Cândido-Bacani[a,b,c], Frédéric Ezan[c], Patrícia de Oliveira Figueiredo[a], Maria de Fátima Cepa Matos[b], Fernanda Rodrigues Garcez[a], Walmir Silva Garcez[a], Georges Baffet[c*]

[a]Instituto de Química, Universidade Federal de Mato Grosso do Sul, Campo Grande, MS, Brazil

[b]Centro de Ciências Biológicas e da Saúde, Universidade Federal de Mato Grosso do Sul, Campo Grande, Brazil

[c] Institut National de la Santé et de la Recherche Médicale (Inserm), UMR1085 Institut de Recherche sur la Santé l'Environnement et le Travail (IRSET); University of Rennes 1, Rennes, France

* Corresponding author:

Institut National de la Santé et de la Recherche Médicale (Inserm), UMR1085 Institut de Recherche sur la Santé l'Environnement et le Travail (IRSET); University of Rennes 1, SFR Biosit, F-35043, Rennes, France

E-mail address: georges.baffet@univ-rennes1.fr and priscila.mcbacani@gmail.com

Highlights

- A novel cyclic peptide identified from *Croton* latex is a candidate for anticancer therapy.
- Crourorb A1 induces apoptosis by caspase-3/7 activation.
- The JNK pathway is involved in crourorb A1-induced hepatocarcinoma cell mortality.

ABSTRACT

[1–9-NαC]-crourorb A1 is a cyclic peptide isolated from *Croton urucurana* Baillon latex, found in midwestern Brazil, that has been shown to exert cytotoxic effects against a panel of cancer cell lines. However, the underlying mechanisms responsible for the crourorb A1-induced cytotoxicity in cancer cells remain unknown. In this study, the effects of crourorb A1 on the viability, apoptosis, cell cycle and migration of Huh-7 (human hepatocarcinoma) cells were investigated. We evaluated the viability of Huh-7 cells treated with crourorb A1 in 2D and 3D collagen cultures and found that cells in 3D culture exhibited increased resistance to crourorb A1 compared to cells in 2D culture (IC_{50}: 62 μg/ml versus 35.75 μg/ml). Crourorb A1 treatment decreases the viability of Huh-7 cells in a dose- and time-dependent manner and is associated with the induction of apoptosis, in the absence of necrotic cells, through the activation of caspase-3/7 and increased expression of the pro-apoptotic proteins Bak, Bid, Bax, Puma, Bim, and Bad. The effects of crourorb A1 are also associated with G2/M phase cell cycle arrest and increases in cyclin-dependent kinase (CDK1) and cyclin B1 expression. A significant reduction in Huh-7 cell migration induced by crourorb A1 was also observed in the presence of mitomycin C. Finally, we showed that

the JNK/MAP pathway, but not ERK signaling, is involved in crourorb A1-induced hepatocarcinoma cell mortality.

Key-words: Peptide; *Croton urucurana*; Cell cycle arrest; Apoptosis; Huh-7 cells

1. Introduction

Medicinal plants play an important role in the discovery of novel bioactive compounds for drug development, especially for anticancer therapy (Pan et al., 2012; Cragg and Newman, 2013). Recently, plant-derived cyclic peptides have emerged as therapeutically potent anticancer biomolecules (Yue et al., 2011; Fang et al., 2013; Mishra et al. 2014).

Studies have shown that cyclic peptides from plants exhibit high cytotoxic activity via cell cycle arrest and apoptosis induction in cancer cell lines (Ma et al., 2006; Mishra et al. 2014; Yeu et al., 2011). In addition, cyclic peptides exhibit a wide range of pharmacological properties, including immunomodulatory, antimalarial, antifungal, antibacterial, antiplasmodial, insecticidal and sedative properties (Tan and Zhou, 2006).

Cyclic peptides have been discovered in medicinal plant species of the families Compositae, Caryophyllaceae, Labiatae, Linaceae, Annonaceae, Amaranthaceae, Rubiaceae and Euphorbiaceae (Tan and Zhou, 2006). *Croton urucurana* Baillon, a member of the Euphorbiaceae family, is a plant commonly found in the state of Mato Grosso do Sul in midwestern Brazil, and its latex has been used in folk medicine for treating cancer (Cândido-Bacani et al., 2015).

Our research program aims to discover potential anticancer compounds from plants of midwestern Brazil, specifically in the Cerrado and Pantanal biomes. As part of this

work, we previously isolated a novel cyclic peptide, designated [1–9-NαC]-crourorb A1, from *Croton urucurana* latex and demonstrated its cytotoxic activity against a panel of cancer cell lines (Cândido-Bacani et al., 2015) (Figure 1). However, the underlying mechanisms involved in crourorb A1-mediated cytotoxicity against cancer cells remain unknown.

Considering the therapeutic potential of crourorb A1 and due to lack of information on the cellular and molecular mechanisms responsible for crourorb A1-induced cytotoxicity on cancer cell lines, in the present study, we investigated the effects of crourorb A1 on the viability, apoptosis, cell cycle and migration of Huh-7 cells, a highly proliferative human hepatocarcinoma cell line. We also evaluated the role of crourorb A1 on the viability of cells in compliant and rigid 3D collagen gels and investigated the cell signaling pathways involved in crourorb A1-induced cell mortality.

2. Materials and Methods

2.1 Cell lines and culture

The human hepatocarcinoma cell line Huh-7D12 was obtained from Health Protection Agency Culture Collections (ECACC, European Collection of Cell Cultures nº 01042712). Cells were cultured in DMEM (Gibco, USA) supplemented with 10% fetal calf serum (FCS) and antibiotics (100 IU/ml penicillin and 100 µg/ml streptomycin). The cells were grown in plastic Petri dishes (100 mm, Corning, NY) in a humidified atmosphere with 5% CO_2 at 37° C.

2.2 Materials

The tetrazolium salt WST-1 (4-[3-(4-iodophenyl)-2-(4-nitrophenyl)-2H-5-tetrazolio]-1,3-benzene disulfonate) was obtained from Roche (Meylan, France), a SensoLyte Homogeneous AMC Caspase-3/7 Assay kit was purchased from Anaspec (Le-Perray-en-Yvelines, France). Propidium iodide (PI), Hoechst and dimethyl sulfoxide (DMSO) were obtained from Sigma-Aldrich (St-Quentin-Fallavier, France). Antibodies against phospho-ERK1/2 (Thr202/Tyr204), phospho-p38 MAPK (Thr180/Tyr182), phospho-SAPK/JNK (Thr183/Tyr185), phospho-p70 S6 Kinase (Thr389), phospho-Akt (Ser473), Bad, Puma, Bid, Bax, Bak, Bim, cyclin B1, CDK1 and cyclin D1 were purchased from Cell Signaling Technology (Ozyme, Saint-Quentin-en- Yveline, France). Polyclonal antibodies against cleaved-caspase 3 and hsc-70 (sc-7298) were purchased from Santa Cruz Biotechnology (Tebu-bio, Le-Perray-en-Yvelines, France). The MEK inhibitor U0126 was purchased from Promega (Charbonnières, France) and JNK inhibitor II was purchased from Calbiochem (VWR, Fontenay-sous-Bois, France). Secondary antibodies conjugated to horseradish peroxidase were obtained from Dako (Trappes, France). Secondary antibodies coupled with Alexa Fluor were obtained from Becton Dickinson (BD Biosciences, San Jose, CA). Cisplatin was obtained from Mylan (Saint-Priest, France) and was used as a positive control. [1–9-NαC]-Crourorb A1 was isolated and identified from *Croton urucurana* Baillon latex at the Institute of Chemistry, Federal University of Mato Grosso do Sul (UFMS), Campo Grande, Brazil (Cândido-Bacani et al., 2015). Crourorb A1 was initially diluted in DMSO, aliquoted and stored at -20°C. The concentration of DMSO in the culture medium was kept below 0.2% (v/v), a concentration known to have no effect on cell viability.

2.3 3D collagen culture

Huh-7 cells were seeded into type I collagen gels (Sigma-Aldrich, St-Quentin-Fallavier, France) diluted with culture medium to obtain a collagen solution of 0.75 mg/ml or 1.5 mg/ml. The pH of the collagen solution was adjusted to 7.4 by 0.1 N NaOH, and the cell suspension was mixed with this solution to give a final cell density of 40.10^3 cells/ml. Collagen gels were then distributed into 96-well plates (100 µl) or 48-well plates (250 µl) and incubated at 37°C. After polymerization (10 min at 37°C), the gels were covered with an equal volume of culture medium.

2.4 Cell viability assay

The viability of Huh-7 cells was evaluated by colorimetric WST-1 assay (Roche, Germany). This assay is based on the ability of viable cells to cleave the sulfonated tetrazolium salt WST-1 (4-[3-(4-iodophenyl)-2-(4-nitrophenyl)-2H-5-tetrazolio]-1,3-benzene disulfonate) by mitochondrial dehydrogenases. Briefly, cells were seeded in 96-well plates in 2D (8×10^3) or 3D collagen gels (4×10^3). Cells in 2D cultures were treated with increasing concentrations of crourorb A1 (0.35-200 µg/ml) or 0.2% DMSO as a control for 24, 48, and 72 h, while 3D-cultured cells were maintained for 6 days, then treated with 10-100 µg/ml crourorb A1 or 0.1% DMSO for 24 h. After treatments, 100 µl of the WST-1 reagent solution (10% in culture medium) was added to each well and incubated for 2 h at 37°C (2D) or for 1 h at 37°C (3D). The absorbance was measured at 430 nm on a SPECTROstar Nano microplate reader (BMG Labtech, Champigny sur Marne, France), and the percentage of viability was calculated as the absorbance ratio of treated to untreated cells. The concentration that inhibited cell growth by 50% (IC_{50}) was determined by a non-linear regression analysis.

2.5 Necrosis study

Huh-7 cells were plated on 35-mm Petri dishes and treated with 36 µg/ml crourorb A1 or 0.036% DMSO as a control for 24 and 48 h. At the indicated times, the medium was removed, and the cells were washed twice with PBS and stained with 5µg/ml Hoechst Stain solution and 5µg/ml propidium iodide at 37° C for 30 min in the dark. After the cells were washed with PBS, 3 drops of fluorescein diacetate (FDA) were added, and the Petri dishes were covered with coverslips and observed by fluorescence microscopy (ZEISS Axio Scope.A1). The doubled-stained nuclei, corresponding to necrotic cells, were counted, and the results are shown as the mean percentages of necrotic cells.

2.6 Caspase-3/7 activity

Caspase-3/7 activity was measured using a SensoLyte Homogeneous AMC Caspase-3/7 Assay kit (Anaspec, Le-Perray-en-Yvelines, France) following the manufacturer's instructions. Briefly, Huh-7 cells were seeded in 96-well plates in 2D culture at a density of 8 x 10^3 cells/well and treated with increasing concentrations of crourorb A1 (10-50 µg/ml) or 0.05% DMSO as a control for 24 h. At the indicated times, cells were lysed on the plate, and the caspase-3/7 substrate solution was incubated with the cell lysates for 1 h at 37°C. AMC cleavage was monitored by spectrofluorometry (Vmax). WST-1 assays were performed in parallel to assess the approximate number of viable cells in each well. Cisplatin (20 µg/ml) was used as a positive control.

2.7 Cell cycle analysis

Huh-7 cells (3×10^5) were seeded in 6-well culture plates and incubated overnight. The next day, cells were treated with 36 or 50 µg/ml crourorb A1 or 0.05% DMSO as a

control for 24 h. Cells were fixed with 70% ice-cold ethanol for 1 h and incubated for 30 min at 37° with 0.5 U RNase A (Sigma-Aldrich). The DNA was then stained for 10 min with 50 µg/ml PI in the dark and subjected to flow cytometric analysis using an FC500 flow cytometer (Beckman Coulter, Paris, France). The percentages of cells in G0/G1, S and G2/M phases were determined using the KALUZA 1.3 analysis software (Beckman Coulter).

2.8 Western blot analysis

Huh-7 cells were treated with 36 µg/ml crourorb A1 or 0.036% DMSO as a control for different lengths of time. Cells were washed with ice-cold PBS, scraped and frozen at -20°C. The protein lysates were separated by sodium dodecyl sulfate–polyacrylamide gel electrophoresis (SDS–PAGE) and transferred to nitrocellulose membranes. The membranes were blocked with 5% low-fat milk in Tris-buffered saline (TBS; 65 mM Tris [pH 7.4], 150 mM NaCl) for 1 h at room temperature, incubated with primary antibodies overnight at 4°C and then incubated with appropriate secondary antibodies linked to horseradish peroxidase in 5% low-fat milk in TBS for 1 h at room temperature. Proteins were visualized with the Immobilon Western Chemiluminescent HRP substrate (VWR) and scanned with the Fujifilm LAS- 3000 imager (Fujifilm, Tokyo, Japan). Densitometric analyses of the bands were performed using the MultiGauge software (Fujifilm).

2.9 Wound-healing assay

Huh-7 cells were seeded in 12-well plates at a density of $1x10^5$ cells/well and grown to 90% confluency at 37°C. The culture medium was discarded, and the scratch-wound assay was performed by scratching the cells with a sterile 200 µl pipet tip. Cells

were then washed twice with PBS to remove the scratched cells. Huh-7 cells were cultured in the absence or presence of 1 µg/ml mitomycin C and treated with 36 µg/ml crourorb A1 or 0.036% DMSO as a control for 24, 48 and 72 h after the scratching. The initial wounding and subsequent migration of the cells in the scratched area were photographed in four different fields under a microscope (AXIOVERT 40 C Zeiss). The results are presented as the percentage width of the gap against the value of the negative control at 0 h of crourorb A1 treatment.

2.10 Cell staining

Huh-7 cells (2D) were seeded in 12-well plates and treated with 50 µg/ml crourorb A1 or 0.050% DMSO as a control for 24 h. The culture medium was removed, and the cells were washed twice with PBS, fixed in 4% paraformaldehyde for 20 min, rewashed, permeabilized in 0.1% Triton X-100/PBS for 10 min, and blocked in PBS/2% BSA for 1 h at room temperature. The slides were stained with 66 nmol/L Phalloidin-FluoProbes 457H (Interchim) and 5 µg/ml Hoechst Stain solution and observed by fluorescence microscopy (Nikon Eclipse Ni).

Growth kinetics of the spheroids (3D) were followed after 4 days of culture and 48 h after treatment with 62 µg/ml crourorb A1 or 0.062% DMSO as a control, and morphological changes were assessed by fluorescent dye labeling. The culture medium was removed, and the cells were washed twice with PBS, fixed in 4% paraformaldehyde for 20 min, rewashed, incubated with PBS containing 50 µM RS19 for 20 minutes and observed with a Leica TCS SP2 confocal scanning head coupled to a DMIRB inverted microscope (Leica Microsystems, Mannheim, Germany). The RS19 dye is a chemical

analog of the voltage sensitive dye Di-6-ASPBS that accumulates in membranes (Rouède et al., 2014).

In addition, collagen gels were dehydrated with successive alcohol and xylene baths with increasing concentrations before being impregnated with paraffin using EXCELSIOR ES tools (Thermo Scientific, Waltham, USA) overnight. After impregnation, gels were embedded in paraffin blocks, and 4-µm-thick sections were cut and stained with hematoxylin and eosin.

2.11 Statistical analysis

Results are expressed as the mean ± standard deviation. The data were analyzed with two-tailed Student's t-test. Differences were considered significant when $p<0.05$ (*), $p<0.01$ (**), $p<0.001$ (***). All experiments were performed at least three times**.**

3. Results

3.1 Effect of crourorb A1 on hepatic cell viability

The *in vitro* cytotoxicity of crourorb A1 against Huh-7 cells was assessed by WST-1 assay. Crourorb A1 decreased the viability of Huh-7 cells in a dose- and time-dependent manner, with the cell viability decreasing with both increased concentrations and incubation times (24, 48 and 72 h). As shown in Figure 2A, treatment with 50, 100 and 200 µg/ml crourorb A1 led to an obvious inhibition in cell viability after only 24 h ($p<0.01$). The effects were maintained and were more pronounced after 48 and 72 h of treatment. With lower crourorb A1 concentrations (0.35, 3 and 12.5 µg/ml), little or no influence on cell viability was observed.

We also treated cells with a wide range of concentrations of crourorb A1 (10 µg/ml to 70 µg/ml) for 24 h. The concentrations of 30, 40, 50 and 70 µg/ml reduced the cell viability to 80%, 20%, 13% and 8% after 24 h of treatment, respectively ($p<0.01$) (Figure 2B). The dose-response curves were used to determine the crourorb A1 concentrations required to inhibit the growth of cancer cells by 50% (IC_{50}). The IC_{50} values at 24, 48 and 72 h were found to be 35.75±1.00, 30.41±2.14 and 20.07±3.40 µg/ml, respectively (Table 1). The IC_{50} value for 24 h of treatment with crourorb A1 was used as an effective concentration for subsequent assays in 2D cultures.

Mechanical forces could greatly influence the viability of hepatoma cells. *In vitro*, 3D collagen gels provide a valuable flexible model for studying cells in a 3D environment and the response to variations of stiffness. This approach allowed us to establish that rigidity could influence the phenotype of hepatoma cells embedded in the matrix (Bomo et al., 2015). In this work, we show that the 3D environment in collagen gels can also influence the response of the cells to crourorb A1, and an increase in cell viability in 3D gels was observed following treatment with 50 and 100 µg/ml crourorb-A1 (Figure 3). The IC_{50} values at 24 h were 62.10±4.70 µg/ml and 62.52±3.12 µg/ml in collagen gels at 0.75 mg/ml (1Pa) and 1.5 mg/ml (3.5Pa), respectively (Table 2), which are 1.8-fold higher than the IC_{50} values identified in 2D culture.

To observe the cluster organization of crourorb A1-treated Huh7 spheroids, we performed 3D confocal imaging and hematoxylin and eosin staining of the spheroids. Z-stack reconstructions of crourorb A1-treated spheroids in three dimensions (xyz) exhibited dramatic changes in cell morphology and the size of spheroids. After 48 h of treatment, these morphological changes showed highly disorganized spheroids with more or less connected cells (Figure 4A-B). These results were confirmed by hematoxylin and eosin

staining (Figure 4C-D). Changes in cell area were measured in crourorb A1-treated cells after 8, 24, 32 and 48 h of treatment in 3.5Pa (1.5 mg/ml) collagen gel. The results indicated that the spheroid surface area decreased by 45% after 48 h of treatment with crourorb A1 compared to control DMSO-treated cells (Figure 4E).

3.2 Crourorb A1 inhibits cell migration and induces G2/M cell cycle phase arrest and apoptosis.

The effects of crourorb A1 on cell motility were examined using a monolayer wound-healing assay. As shown in Figure 5, wound closure was markedly delayed in crourorb A1-treated cells compared to control DMSO-treated cells, whether the cells were cultured in the presence or absence of mitomycin C (Figures 5A-C). Mitomycin C is an antibiotic that is highly effective against various types of human cancers and is capable of blocking mitosis and inhibiting cancer cell growth. These results revealed that crourorb A1 could inhibit the migration of Huh-7 cells in a time-dependent manner ($p<0.05$) independent of possible cell cycle effects.

To determine the influence of crourorb A1 on cell cycle progression, flow cytometry analysis was performed and G0/G1, S and G2/M cell cycle phases were detected by PI staining. Our results showed a dose-dependent increase in cells in G2/M phase after treatment with 36 and 50 μg/ml crourorb A1 for 24 h (Figure 6A and B), while the percentage of cells in G0/G1 phase was significantly decreased ($p<0.01$) (Figure 6B). To better understand the mechanisms of crourorb A1-induced G2/M arrest, we examined the expression of G2/M and G1 phase-related regulatory proteins by Western blot. As shown in Figure 6C, the expression level of Cdk1 (cyclin-dependent kinase 1), cyclin B1 and cyclin D1 increased in Huh-7 cells in a time-dependent manner. A slight decrease in Cdk1

expression can be observed after 48 h of treatment. An increase of P53 expression after 24h of crourorb A1 treatment can be noticed (figure 6D).

We analyzed the morphological alterations of nuclei after treatment with 50 µg/ml crourorb A1 for 24 h and observed an increase of apoptotic cells with characteristic apoptotic nuclei stained by Hoechst compared to control cells (Figure 7A). Figure 7B shows the percentage of necrotic cells after 24 h and 48 h of treatment with crourorb A1 at the IC_{50} dose (36 µg/ml). As shown in Figure 7B, there were no significant differences compared to the DMSO control, and only basal levels of necrotic cells could be observed.

To evaluate whether the inhibition of the cell viability in response to crourorb A1 was due to the induction of apoptosis, caspase-3/7 activity was measured. Treatment of Huh-7 cells with crourorb A1 at 30, 40 and 50 µg/ml for 24 h resulted in significantly increased caspase-3/7 activity compared to control cells (Figure 7C) ($p<0.05$; $p<0.001$). At higher concentrations (70 µg/ml), crourorb A1 did not induce significant caspase-3/7 activity because of its high cytotoxicity, which led to considerable cell death (data not shown). Since the pro-apoptotic Bcl-2 family is the principal pathway involved in apoptosis, the levels of Bak, Bad, Puma, Bax, Bim, Bid and the cleaved-caspase-3 protein were analyzed by Western blot after 10, 24 and 48 h of treatment with crourorb A1. The results showed that the levels of all the pro-apoptotic proteins analyzed increased in crourorb A1-treated cells. Similar results were also observed in the levels of cleaved caspase-3 in crourorb A1-treated cells after 24 and 48 h of treatment (Figure 7D).

3.3 The JNK pathway but not MEK/ERK is involved in the mortality induced by crourorb A1

The phosphorylation level of the MAP kinases ERK1/2, JNK and p38 and proteins AKT and p70 S6 kinase (p70S6K) was analyzed in Huh-7 cells treated with crourorb A1 at the IC_{50} dose of 36 µg/ml for 10 min, 30 min, 3 h, 6 h, 10 h, 24 h and 48 h. As shown in Figure 8A, crourorb A1 stimulated the phosphorylation of AKT after 3 h of treatment with a slow increase thereafter until 48 h. Early phosphorylation of ERK1/2 was observed in control (DMSO) and crourorb A1-treated cells, whereas ERK1/2 activation after 10 h was specific to the crourorb A1-treated cells. This activation lasted until 48 h in a time-dependent manner compared to the control. Interestingly, phosphorylation of JNK peaked at 30 min and was still clearly detected 10 h after the stimulation (Figure 8A) of crourorb A1 treatment. The phosphorylation of p70S6K and p38 was not greatly influenced by crourorb A1 during the time course analyzed compared to the control cells.

To study the role of the ERK1/2 and JNK pathways in crourorb A1-mediated survival/cytotoxicity, we analyzed the effect of the inhibition of these pathways on cell viability by WST-1 assay. As shown in Figure 8B, no significant changes in cell viability were detected after treatment with U0126, a MEK inhibitor ($p>0.05$). In contrast, there was a blockage of crourorb A1 toxicity in cells treated with the JNK inhibitor, indicating that JNK signaling could be a key pathway involved in crourorb A1-induced cell mortality (Figure 8C). To demonstrate the effectiveness of the inhibitors, we analyzed the phosphorylation of JNK and ERK1/2, which was largely to totally abolished by JNK inhibitor II and U0126, respectively. Interestingly, JNK inhibition decreased cyclin D1 and Cdk1 expressions showing that this inhibition in presence of crourorb could have an impact on the cell cycle regulation. Furthermore, we did not detect any activation of P-ERK and P-AKT after JNK inhibition (figure 8D).

4. Discussion

Crourorb A1, a novel cyclic peptide isolated from the medicinal *Croton urucurana* Baillon latex (Brazil), has previously been identified as a candidate anticancer agent due its potential cytotoxic effects against a panel of human cancer cell lines (Cândido-Bacani et al., 2015). However, the cellular and molecular mechanisms responsible for crourorb A1-induced cytotoxicity on cancer cell lines have not been investigated. In the present study, we determined the cytotoxic effects of crourorb A1 on Huh-7 cells and demonstrated that treatment of Huh-7 cells with crourorb A1 induced apoptosis, arrested the cell cycle in G2/M phase and inhibited cell motility. We also demonstrated the effect of crourorb A1 on the viability of Huh-7 cells grown in 3D collagen gels.

The cytotoxicity of crourorb A1 in Huh-7 cells was detected by WST-1 assay, and results indicated that crourorb A1 decreased cell viability in a dose- and time-dependent manner. Crourorb A1 concentrations in the range of 50–200 μg/ml reduced cell viability; however, no alteration in the viability was observed with lower crourorb A1 concentrations (0.35 and 12.5 μg/ml) after 24, 48 and 72 h of exposure. The IC_{50} value (30.41 μg/ml) of 48 h of crourorb A1 treatment in Huh-7 cells corroborated the results reported in our previous study (Cândido-Bacani, 2015), which showed that concentrations ranging from 29 to 41 μg/ml inhibited by 50% the viability of HT-29 (colon carcinoma), MCF-7 (breast adenocarcinoma), Hep-G2 (hepatocellular carcinoma) and PC-03 (prostate carcinoma) human cancer cells. In contrast, crourorb A1 demonstrated potent cytotoxic activity against adriamycin-resistant ovarian (NCI-ADR/RES) cancer cells (IC_{50} =3.98 μg/ml) and moderate cytotoxicity against human kidney (786-0) cancer cells (IC_{50} =18.69 μg/ml). Additionally, it was shown that crourorb A1 had no effect on non-tumor cell viability (NIH/3T3 murine fibroblast cells) (IC_{50} >250 μg/ml) (Cândido-Bacani et al., 2015). These

results suggest that crourorb A1 may selectively inhibit the viability of cancer cells with differences in responsiveness and sensitivity depending on the cancer cell line, whereas immortalized cells are much less or not at all sensitive to crourorb A1.

Since apoptosis plays a central role in limiting the uncontrolled proliferation of cancer cells (Elmore 2007; Ziegler and Kung, 2008), we investigated the apoptotic effect of crourorb A1 in the highly proliferative hepatocarcinoma cell line Huh-7. Apoptosis is characterized by morphological changes including cell shrinkage, membrane blebbing, DNA fragmentation, chromatin condensation and apoptotic body formation. These changes require the activation of several signaling cascades that are regulated by various cellular proteins (Sprick and Walczak, 2004; Elmore, 2007; Bruin and Medema, 2008; Estaquier et al., 2012), including the Bcl-2 family proteins. Indeed, it has been shown that this family includes pro-apoptotic (Bax, Bak, Bcl-XS, Bid, etc.) and anti-apoptotic (Bcl-2, Bcl-XL, Mcl-1, A1, Bcl-W, etc.) proteins that play an essential role in this mechanism (Burlacu, 2003; Chipuk and Green, 2008; Song et al., 2013). These proteins regulate the permeability of the mitochondrial membrane and promote the activation of different classes of caspases (initiators and effectors), leading to apoptotic cell death (Chipuk and Green, 2008, Song et al., 2013; Czabotar et al., 2014). The caspase family plays a crucial role in the implementation of apoptosis, and caspase activation appears to be linked to the molecular and structural changes that occur during apoptosis. Among the identified caspases, caspase-3 is known to be the major executioner caspase of the apoptotic cell death program (Elmore, 2007). In this study, we observed by fluorescent dye labeling of Huh-7 cells that crourorb A1 caused morphological changes characteristic of apoptosis. Crourorb A1-induced apoptosis was confirmed by an increase in caspase-3/7 activity in a dose-dependent manner, accompanied by the up-regulation of cleaved-caspase3 protein and

expression of pro-apoptotic proteins such as Bak, Bid, Bax, Puma, Bim, and Bad. Taken together, our data show that crourorb A1-induced cytotoxicity could be strongly mediated through a caspase-3-dependent pathway and pro-apoptotic protein up-regulation. The apoptotic effects of natural cyclic peptides, such as jasplakinolide, have also been demonstrated in human leukemia Jurkat T cells by Odaka et al. (2000). Jasplakinolide-induced apoptosis was associated with an increase in caspase-3 activity and Bax levels and accompanied by a decrease in the expression of Bcl-2 in Jurkat T cells (Odaka et al., 2000). Jasplakinolide was also capable of inducing apoptosis in various murine transformed cell lines, including T-cell lymphoma EL-4 cells, myeloma SP-2/0 cells, macrophage-like J774.1 cells and fibroblast L cells (Odaka et al., 2000). Cozzolino et al. (2005) have demonstrated that astins, a family of cyclopentapeptides isolated from the roots of the medicinal plant *Aster tataricus* (Compositae), exhibit potent caspase-dependent pro-apoptotic activity in human papillary thyroid carcinoma cells (NPA cell line). Recently, a new cyclic octapeptide named cyclosaplin showed antiproliferative activity against human breast cancer cells (MDA-MB-231) through the inhibition of cell viability and induction of apoptosis by caspase-3 activation (Mishra et al. 2014).

Additionally, we investigated the effect of crourorb A1 on cell cycle progression. In the present study, we demonstrated that crourorb A1 induced a blockage of cell cycle progression of the Huh-7 cells by the accumulation of cells in G2/M phase. In parallel, we observed that crourorb A1 treatment resulted in an increase in the expression of Cdk1 and cyclin B1. Since the Cdk1/cyclin B1 complex plays an important role in the transition from G2 to M phase (Murray, 2004), here, we suggest that crourorb A1 could increase the proportion of cells in G2/M phase by blocking cells in late G2 and/or beginning of M phase by a mechanism related to an increase in the expression of Cdk1 and cyclin B.

Indeed, natural cyclic peptides have been reported to inhibit cancer cell growth by mediating cell cycle arrest in the G2/M phase in cancer cell lines (Yeu et al., 2011; Du et al., 2014), a feature regarded as an effective strategy for inhibiting cancer cell growth (Zhang et al., 2005). Cell migration is an essential step in cancer progression, leading to invasion and metastasis (Pasco et al., 2004). In our study, we also demonstrated the effects of crourorb A1 on the migration of Huh-7 cells cultured in the absence and presence of mitomycin C. With the use of mitomycin C, it is therefore possible to analyze cell migration in the absence of cell proliferation (Mao et al., 1999; Gen et al., 2009). Crourorb A1 treatment was shown to inhibit the migration potential of Huh-7 cells by wound-healing analysis both in the absence and presence of mitomycin C, excluding the possibility that the effect of crourorb A1 on cell migration could be a consequence of its inhibition of cell proliferation.

The MAPK pathways play a key role in cell migration, survival/apoptosis and proliferation (Chang et al., 2003; Le et al., 2003; Dhillon et al., 2007; Zang et al., 2011; Hein et al., 2014). Thus, we analyzed the phosphorylation state of the MAP kinases p38, ERK and JNK and of the proteins AKT and p70S6K in response to crourorb A1. We showed that the JNK, ERK1/2 and AKT pathways were activated in a time-dependent manner after crourorb A1 exposure, whereas the phosphorylation levels of p38 and p70S6K were not affected, compared to control cells treated with solvent (DMSO). Moreover, we determined that the JNK pathway was necessary for crourorb A1-induced cell death, as evidenced by the protection against crourorb A1-induced apoptosis conferred by the JNK inhibitor II. On the other hand, although crourorb A1 activated the ERK1/2 pathway, the inhibitor U0126 was not effective in preventing crourorb A1-induced cell death, indicating that the activation of ERK1/2 seems not involved in the cytotoxic effects

of crourorb A1 in Huh-7 cells. The regulation via JNK seems to be complex. In fact, JNK inhibition did not decrease Bim apoptosis-related protein level but rather increase the level (result not shown), but slightly decrease P53 expression. However, JNK inhibition decreased cyclin D1 and Cdk1 expressions indicating that this inhibition in presence of crourorb could have an impact on the cell cycle regulation.

Based on the knowledge that 3D cultures better approximate the *in vivo* environment and can lead to divergent results when compared to 2D cultures (Mikhail et al., 2013; Eicheler et al., 2014), we quantified the viability of 3D-cultured cells, in stiff and soft matrix, after crourorb A1 treatment. Huh-7 cells in these matrices exhibited changes in morphology and proliferation. In soft collagen gels (0.75 mg/ml collagen), Huh-7 cells appear well spread and form monolayer-like structures with flattened shapes, while in rigid gels (1.5 mg/ml collagen), cells do not spread and rapidly form spherical clusters during culture (Bomo et al., 2015). In our study, we showed that cells grown in 3D collagen gels exhibited increased resistance to crourorb A1 when compared to 2D cell culture; however, no difference was observed between the two 3D culture models. IC_{50} values were 1.8-fold higher in both 3D models compared to conventional 2D monolayer cultures. Similar results were obtained for the positive control cisplatin. Moreover, 3D reconstruction of spheroids treated with crourorb A1 showed significant morphological alterations and decreases in cell surface area when compared to untreated cells. These data are in accordance with previous studies that also showed a greater resistance to the anti-cancer drug in 3D cultures in comparison to 2D-cultured cells (Yip and Cho, 2013; Godugo et al., 2013; Mikhail et al., 2013; Eicheler et al., 2014; Lauer et a.,2014). This resistance to anticancer drugs in 3D models has been attributed to several mechanisms, including a “decreased penetration of anticancer drugs, increased pro-survival signaling, and/or upregulation of genes conferring

drug resistance" (Godugo et al., 2013). In addition, it is thought that the spheroids have the "ability to block the diffusion of the drug to all the cells as cells on the outer layers of the spheroid provide a natural barrier" (Yip and Cho, 2013). However, the Huh-7 spheroids appear as acini-like structures with hollow lumen, weakening the drug accessibility hypothesis (Bomo et al, 2015).

In conclusion, our data suggest that exposure of Huh-7 cells to crourorb A1, a cyclic peptide, resulted in decreased cell viability mediated by G2/M cell cycle arrest and the consequent induction of apoptosis. Furthermore, crourorb A1 inhibited cell migration. We also demonstrated that the JNK pathway is involved in the mechanism of crourorb A1-induced cell death in Huh-7 cells.

Conflicts of interest

The authors declare that there are no conflicts of interest.

Acknowledgments

The authors wish to thank Fundect-MS, CNPq, and CPq-PROPP-UFMS for their financial support and CAPES Foundation, Ministry of Education of Brazil for the doctoral grants awarded to P.M. Cândido-Bacani (Proc. nº 99999.002264/2014-05), and the French Institut National de la Santé et de la Recherche Médicale (Inserm) and the University of Rennes 1 for financial support. Thanks are also extended to Dr M. Blanchard-Desce (UMR CNRS 5255, University of Bordeaux, France), who kindly provided us with fluorescent dye RS19 and the PIXEL, flow cytometry and H2P2 platforms (SFR Biosit, UMS CNRS 3480 /US INSERM 018, Rennes).

References

Bomo, J., Ezan, F., Tiaho, F., Bellamri, M., Langouët, A., Theret, N., Baffet, G., 2015. Increasing 3D Matrix Rigidity Strengthens Proliferation and Spheroid Development of Human Liver Cells in a Constant Growth Factor Environment. J. Cell. Biochem. 9999, 1–13.

Bruin, E. C., Medema, J. P., 2008. Apoptosis and non-apoptotic deaths in cancer development and treatment response. Cancer Treat. Res. 34, 737–749.

Cândido-Bacani, P. M., Figueiredo, P. O., Matos, M. F. C., Garcez, F. R., Garcez, W. S., 2015. Cytotoxic orbitide from the latex of Croton urucurana. J. Nat. Prod. 78, 2754−2760.

Chang, F., Steelman, L. S., Lee, J. T., Shelton, J. G., Navolanic, P. M., Blalock, W. L., Franklin, R. A., McCubrey, J. A., 2003. Signal transduction mediated by the Ras/Raf/MEK/ERK pathway from cytokine receptors to transcription factors: potential targeting for therapeutic intervention. Leukemia 17, 1263–1293.

Chipuk, J. E., Green, D. R. 2008. How do Bcl-2 proteins induce mitochondrial outer membrane permeabilization? Trends Cell Biol. 18, 157-164.

Cozzolino, R., Palladino, P., Rossi, F., Calı, G., Benedetti, E., Laccetti, P., 2005. Antineoplastic cyclic astin analogues kill tumour cells via caspase-mediated induction of apoptosis. Carcinogenesis 26, 733-739.

Cragg, G. M., Newman, D. J., 2013. Natural products: A continuing source of novel drug leads. Biochim. Biophys. Acta 1830, 3670–3695.

Czabotar, P. E., Lessene, G., Strasser, A., Adams, J. M., 2014. Control of apoptosis by the BCL 2 protein family: implications for physiology and therapy. Nat. Rev. Mol. Cell Bio. 15, 49-63.

Dhillon, A. S., Hagan, S., Rath, O., Kolch, W., 2007. MAP kinase signalling pathways in cancer. Oncogene 26, 3279–3290.

Du, L., Risinger, A. L., King, J. B., Powell, D. R., Cichewicz, R. H., 2014. A potent HDAC inhibitor, 1‐Alaninechlamydocin, from a Tolypocladium sp. induces G2/M cell cycle arrest and apoptosis in MIA PaCa‐2 Cells. J. Nat. Prod. 77, 1753-1757.

Eichler, M., Jahnke, E.-G., Krinke, D., Müller, A., Schmidt, S., Azendorf, R., Robitzki, A. A., 2014. A novel 96-well multi electrode array based impedimetric monitoring platform for comparative drug efficacy analysis on 2D and 3D brain tumor cultures. Biosens. Bioelectron.15, 582-589.

Elmore, S., 2007. Apoptosis: A review of programmed cell death Toxicol. Pathol. 35, 495–516.

Estaquier, J., Vallette, F., Vayssiere, J.-L., Mignotte, B., 2012. The mitochondrial pathways of apoptosis. Adv. Exp. Med. Biol. 942, 157-183.

Fang, X.-W., Chen, W., Fan, J.-T., Song, R., Wang, L., Gu, Y.- H., Zeng, G-. Z., Shen, Y., Wu, X.-F., Tan, N.- H., Xu, Q., Sun, Y., 2013. Plant cyclopeptide RA-V kills human breast cancer cells by inducing mitochondria-mediated apoptosis through blocking PDK1–AKT interaction. Toxicol. Appl. Pharm. 267, 95–103.

Gen, Y., Yasui, K., Zen, K., Nakajima, T., Tsuji, K., Endo, M., Mitsuyoshi, H., Minami, M., Itoh, Y., Tanaka, S., Taniwaki, M., Arii, S., Okanoue, T., Yoshikawa, T., 2009. A novel amplification target, ARHGAP5, promotes cell spreading and migration by negatively regulating RhoA in Huh-7 hepatocellular carcinoma cells. Cancer Lett. 275, 27–34.

Godugu, C., Patel, A. R., Desai, U., Andey, T., Sams, A., Singh, M., 2013. AlgiMatrixTM based 3D cell culture system as an in vitro tumor model for anticancer studies. PloS one 8, e53708.

Hein, A. L., Ouellette, M. I. M., Yan, Y., 2014. Radiation-induced signaling pathways that promote cancer cell survival (Review). Int. J. Oncol. 45, 1813-1819.

Lauer, F. M., Kaemmerer, E., Meckel, T., 2014. Single molecule microscopy in 3D cell cultures and tissues. Adv. Drug Deliv. Rev. 79-80, 79-94.

Le, X.-F., Hittelman, W. N., Liu, J., Watters, A. M., Li, C., Mills, G. B., Bast Jr, R. C., 2003. Paclitaxel induces inactivation of p70 S6 kinase and phosphorylation of Thr421 and Ser424 via multiple signaling pathways in mitosis. Oncogene 22, 484–497.

Ma, X., Wu, C., Wang, W., Li, X., 2006. Peptides from plants: a new source for antitumor drug research. Asian J. Tradit. Med. 1 (2) 85-90.

Mao, Y., Varoglu, M., Sherman, D. H., 1999. Genetic localization and molecular characterization of two key genes (mitAB) required for biosynthesis of the antitumor antibiotic mitomycin C. J. Bacteriol. 181, 2199–2208.

Mikhail, A. S., Eetezadi, S., Allen, C., 2013. Multicellular Tumor spheroids for evaluation of cytotoxicity and tumor growth inhibitory effects of nanomedicines in vitro: a comparison of docetaxel- loaded block copolymer micelles and taxotere. PloS one 8, e62630.

Mishra, A., Gauri, S. S., Mukhopadhyay, S. K., Chatterjee, S., Das, S. S., Mandal, S. M., Dey, S., 2014. Identification and structural characterization of a newpro-apoptotic cyclic octapeptide cyclosaplin fromsomatic seedlings of Santalum album L. Peptides 54, 148–158.

Murray, A. W., 2004. Recycling the cell cycle: review cyclins revisited. Cell 116, 221–234.

Odaka, C., Sanders, M. L., Crews, P., 2000. Jasplakinolide induces apoptosis in various transformed cell lines by a Caspase-3-like protease-dependent pathway. Clin. Diagn. Lab. Immunol. 7, 947–952.

Pan, L., Chai, H.-B., Kinghorn, A. D., 2012. Discovery of new anticancer agents from higher plants. Front. Biosci. (Schol. Ed.) 4, 142–156.

Pasco, S., Ramont, K., Maquart, F.-X., Monboisse, J. C., 2004. Control of melanoma progression by various matrikines from basement membrane macromolecules. Crit. Rev. Oncol. Hematol. 49, 221–233.

Rouède D, Coumailleau P, Schaub E, Bellanger JJ, Blanchard-Desce M, Tiaho F., 2014. Myofibrillar misalignment correlated to triad disappearance of mdx mouse gastrocnemius muscle probed by SHG microscopy. Biomed Opt Express. 5(3):858-75.

Song, J., Hou, L., Ju, C., Zhang, J., Ge, Y., Yue, W., 2013. Isatin inhibits proliferation and induces apoptosis of SH-SY5Yneuroblastoma cells in vitro and in vivo. Eur. J. Pharmacol. 702, 235–241.

Sprick, M. R., Walczak. H., 2004. The interplay between the Bcl-2 family and death receptor-mediated apoptosis. Biochim. Biophys. Acta 1644, 125-132.

Tan, N.-H., Zhou, J., 2006. Plant cyclopeptides. Chem. Rev. 106, 840-895.

Watters, D. J., Beamish, H. J., Marshall, K. A., Gardiner, R. A., Seymour, G. J., Lavin, M. F., 1994. Accumulation of HL-60 leukemia cells in G2/M and inhibition of cytokinesis caused by two marine compounds, bistratene A and cycloxazoline. Cancer Chemother. Pharmacol. 33, 399-409.

Yip, D., Cho, C. H., 2013. A multicellular 3D heterospheroid model of liver tumor and stromal cells in collagen gel for anti-cancer drug testing. Biochem. Biophys. Res. Commun. 433, 327–332.

Yue, G. G. L., Fan, J-. T., Lee, J. K. M., Zeng, G. Z., Ho, T. W. F., Fung, K. P., Leung, P. C., Tan, N,-H., Lau, C. B. S., 2011. Cyclopeptide RA-V inhibits angiogenesis by down-regulating ERK1/2 phosphorylation in HUVEC and HMEC-1 endothelial cells. British. J. Pharm. 164, 1883–1898.

Zhang, M., Chen, H., Huang, J., Zhong, L., Zhu, C. P., Zhang, S. H., 2005. Effect of Lycium barbarum polysaccharide on human hepatoma QGY7703 cells: inhibition of proliferation and induction of apoptosis. Life Sci. 76, 2115–2124.

Zhang, X., Tang, N., Hadden, T. J., Rishi, A. R., 2011. Akt, FoxO and regulation of apoptosis. Biochim. Biophys. Acta 1813, 1978–1986.

Ziegler, D. S., Kung, A. L., 2008. Therapeutic targeting of apoptosis pathways in cancer. Current Opinion in Oncology 20, 97–103.

Figure Legends

Figure 1. Chemical structure of [1–9-NαC]-crourorb A1.

Figure 2. Cell viability (%) in 2D cultures was determined by WST-1 assay. (A) Huh-7 cells were treated with increasing concentrations of crourorb A1 (0.35-200 µg/ml) or with 0.2% DMSO as a control for 24, 48 and 72 h. (B) Huh-7 cells were treated with increasing concentrations of crourorb A1 (10-70 µg/ml) or with 0.07% DMSO as a control for 24 h. Results are expressed as the percentage change compared to the control (**$p<0.01$; significantly different from the control).

Figure 3. Cell viability (%) in 3D cultures (0.75 and 1.5 mg/ml collagen gel) was determined by WST-1 assay. Huh-7 cells were treated with increasing concentrations of crourorb A1 (10-100 µg/ml) or with 0.1% DMSO as a control for 24 h after 6 days of culture. Results are expressed as the percentage change compared to the control (**$p<0.01$; significantly different from the control).

Figure 4. Changes in the cluster organization of crourorb A1-treated Huh-7 cells in 3D collagen gel cultures (1.5 mg/ml collagen gel). (A) 3D reconstruction of Huh-7 cells treated with 0.062% DMSO as a control or (B) 62 µg/ml crourorb A1 for 48 h after 4 days of culture in 1.5 mg/ml collagen gel. For fluorescent dye labeling, cells were incubated with PBS containing 50 µM RS19 for 20 minutes. (C) Hematoxylin and eosin staining after paraffin inclusion and observation with a slide scanner of Huh-7 spheroids treated for 48 h with 0.062% DMSO as a control or (D) 62 µg/ml crourorb A1 for 48 h after 4 days of

culture in 1.5 mg/ml collagen gel. (E) Huh-7 cells were treated with 62 µg/ml crourorb A1 or with 0.062% DMSO as a control for 8 h, 24 h, 32 h and 48 h after 4 days of culture and cell surface (area) was measured ($^{**}p<0.01$, $^{***}p<0.001$; significantly different from the control).

Figure 5. Crourorb A1 inhibits migration in 2D-cultured Huh-7 cells. Cells were cultured in the absence (A-B) or presence (C) of mitomycin C and treated with 36 µg/ml crourorb A1 or 0.036% DMSO as a control for 24, 48 and 72 h. The rate of migration was measured by quantifying the total distance that the cells moved from the edge of the scratch toward the center. Values are represented as the mean±SD of three independent experiments (*p<0.05; **p<0.01, relative to those of the control group). Scale bar=100 µm.

Figure 6. Effects of crourorb A1 on cell cycle phase distribution. (A) Representative histograms depicting cell cycle distribution in 2D-cultured Huh-7 cells treated with 36 or 50 µg/ml crourorb A1 or 0.05% DMSO as a control for 24 h; the cell-cycle distribution was analyzed by flow cytometry. (B) The percentage of cells in the G0/G1, S, and G2/M phases of the cell cycle are shown. Huh-7 cells were treated with 36 or 50 µg/ml crourorb A1 or 0.05% DMSO as a control for 24 h. (C) For protein levels, Huh-7 cells were treated with 36 µg/ml crourorb A1 for 10, 24 and 48 h and subjected to Western blot analysis of the expression of CDK-1 and cyclin B1, with Hsc-70 as an internal control. (D) Expression of P53 after 24h of treatment or not with 36 µg/ml crourorb A1. The data are represented as the mean±SD of three independent experiments (**p<0.01).

Figure 7. Effects of crourorb A1 on apoptosis and necrosis. (A) Morphological changes of 2D-cultured Huh-7 cells in the presence or absence of crourorb A1. Huh-7 cells were treated with 50 µg/ml crourorb A1 or 0.05% DMSO as a control for 24 h (magnification x40, scale bar=50 µm). (B) Study of Huh-7 necrosis: cells were stained with Hoechst Stain solution and propidium iodide after 24 h and 48 h of treatment with 36 µg/ml crourorb A1 or 0.036% DMSO as a control. (C) Apoptosis of 2D-cultured Huh-7 cells was determined by caspase-3/7 activity by DEVD-AMC fluorometric assay after 24 h treatment with different concentrations of crourorb A1 (10-50 µg/ml) or 0.05% DMSO as a control. (D) For apoptosis-related proteins levels, Huh-7 cells were treated with 36 µg/ml crourorb A1 for 10, 24 and 48 h and subjected to Western blot analysis with antibodies to different proapoptotic proteins, with Hsc-70 as an internal control. Results are expressed as the mean of three independent experiments (mean±SD; *$p<0.05$; ***$p<0.001$).

Figure 8. Effects of crourorb A1 on cell signaling pathways. (A) 2D-cultured Huh-7 cells were treated with 36 µg/ml crourorb A1 or 0.036% DMSO as a control and arrested at the indicated times to analyze phosphorylated AKT, ERK1/2, JNK, p70S6 and p38 protein levels by Western blot. Hsc-70 served as an internal control. (B and C) Cells were pretreated for 1 h with dimethyl sulfoxide or with the MEK inhibitor U0126 or JNK inhibitor II, then exposed to 36 µg/ml crourorb A1. (B) WST-1 assays were performed after 24 h of co-treatment with U0126 or JNK inhibitor II and crourorb A1. (C) Phosphorylation of ERK1/2 and JNK was monitored by Western blot and Hsc-70 was used as an internal control. (D) Expressions of cyclin D1, Cdk1, P53 and activations of ERK and AKT after JNK inhibition. The data are represented as the mean±SD of three independent experiments (***$p<0.001$).

Figure 9. Scheme showing the biochemical pathways that are activated by crourorb A1 in Huh-7 cells

Figure 1

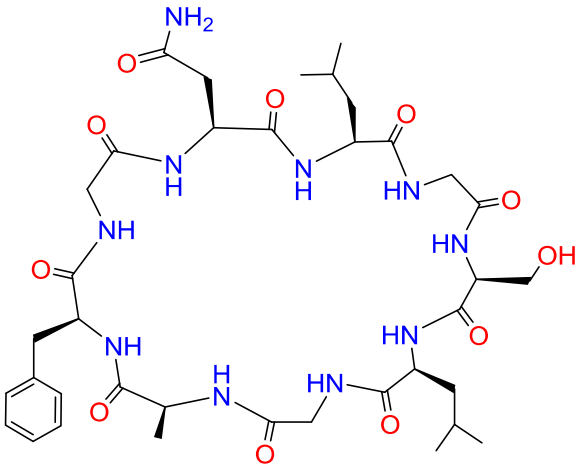

Figure 2

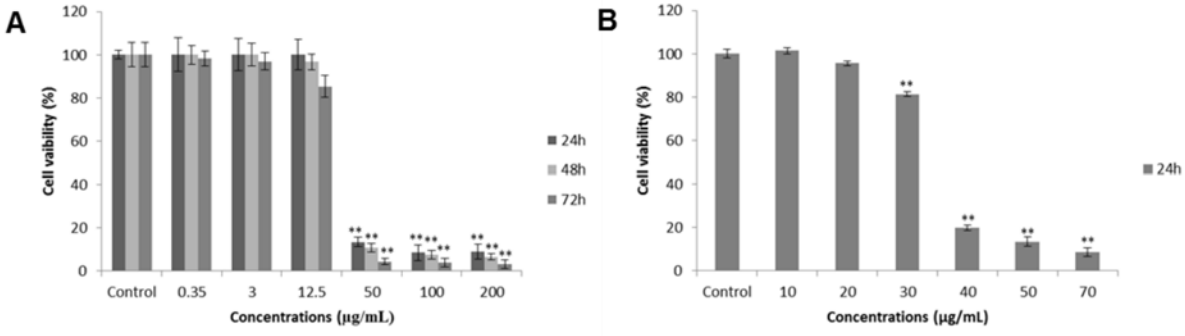

Figure 3

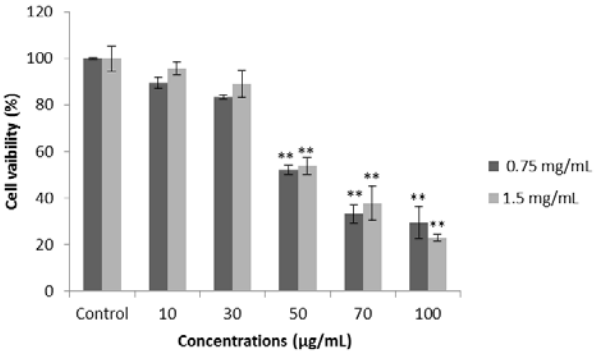

Figure 4

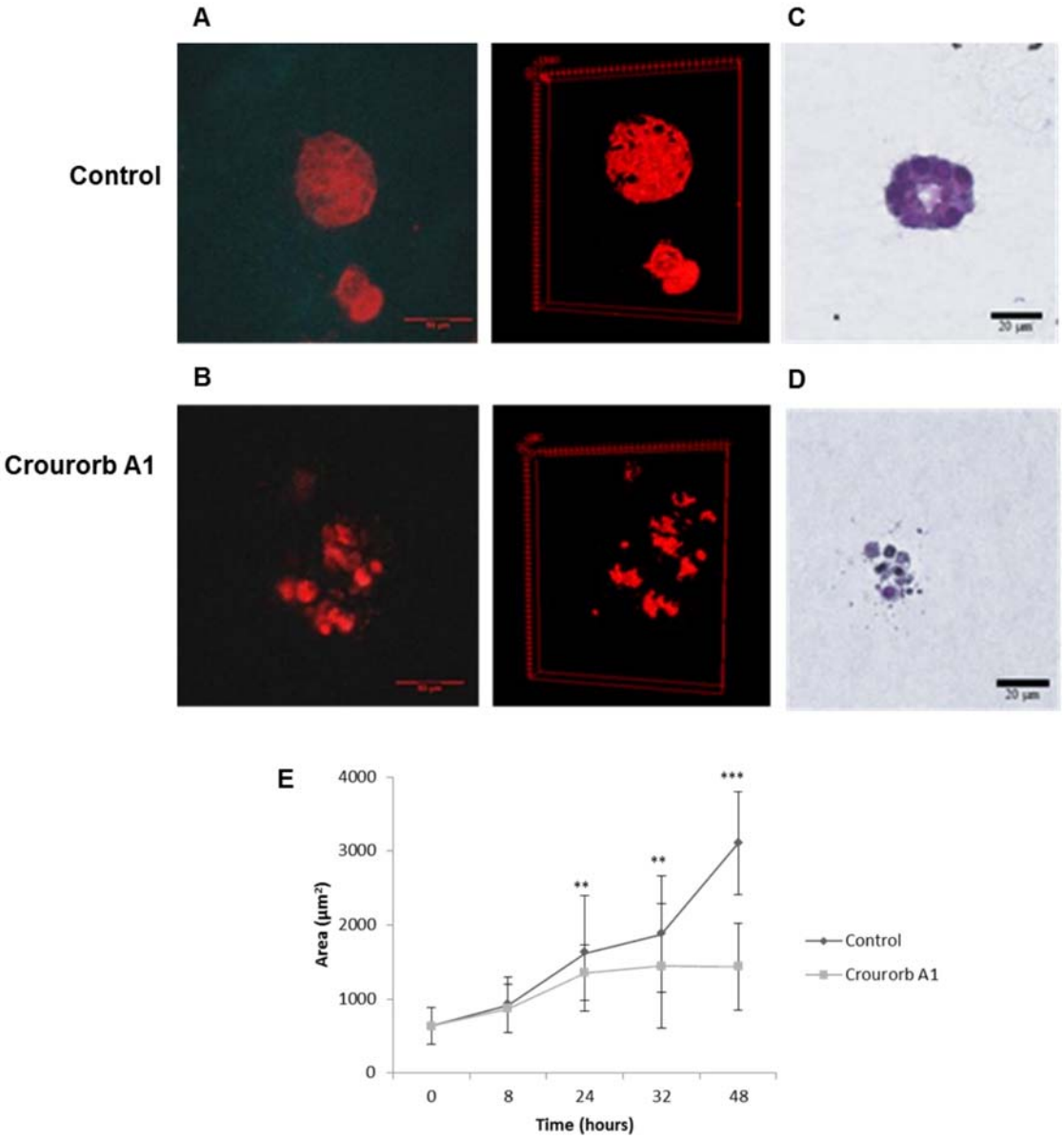

Figure 5

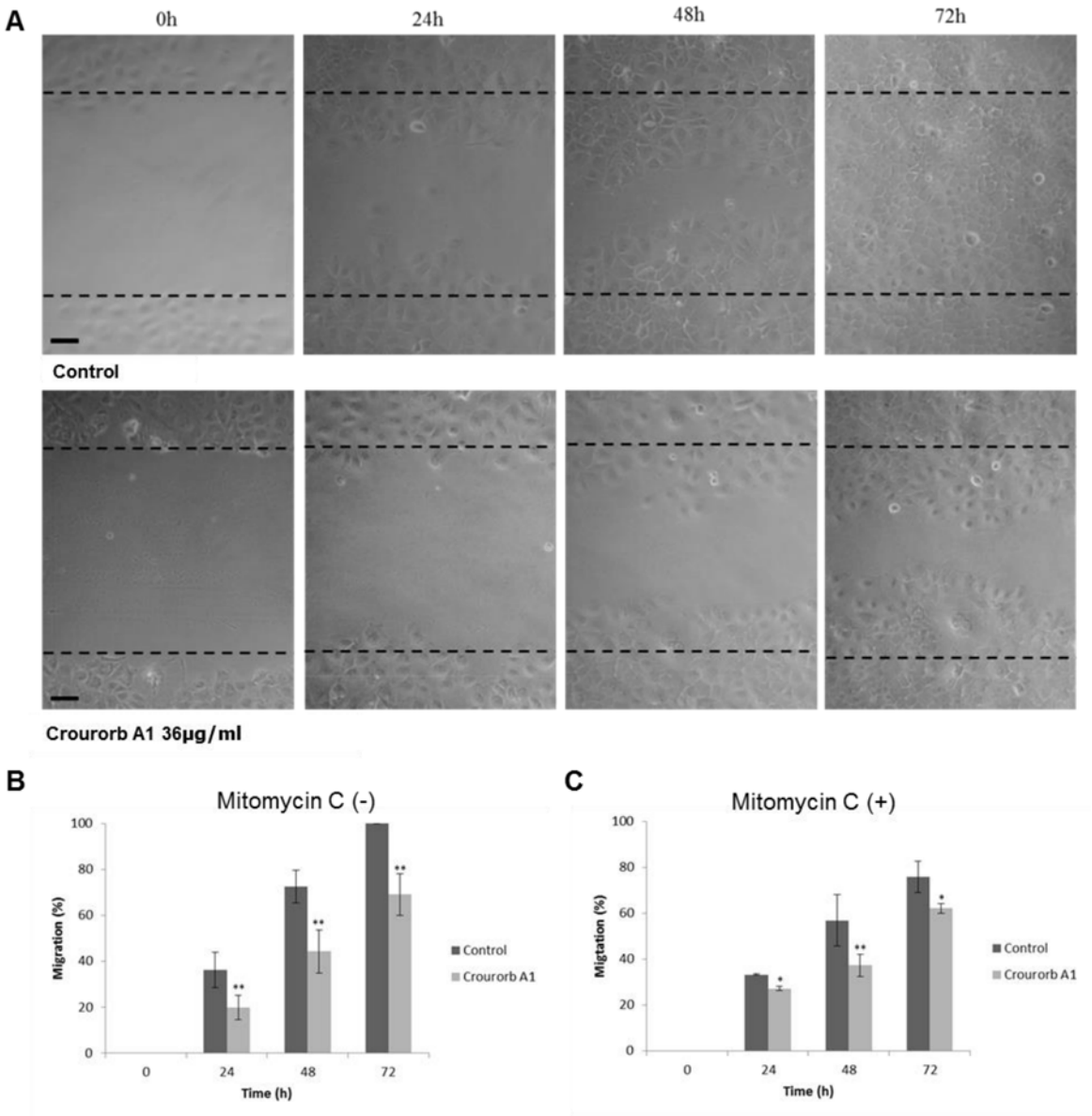

Figure 6

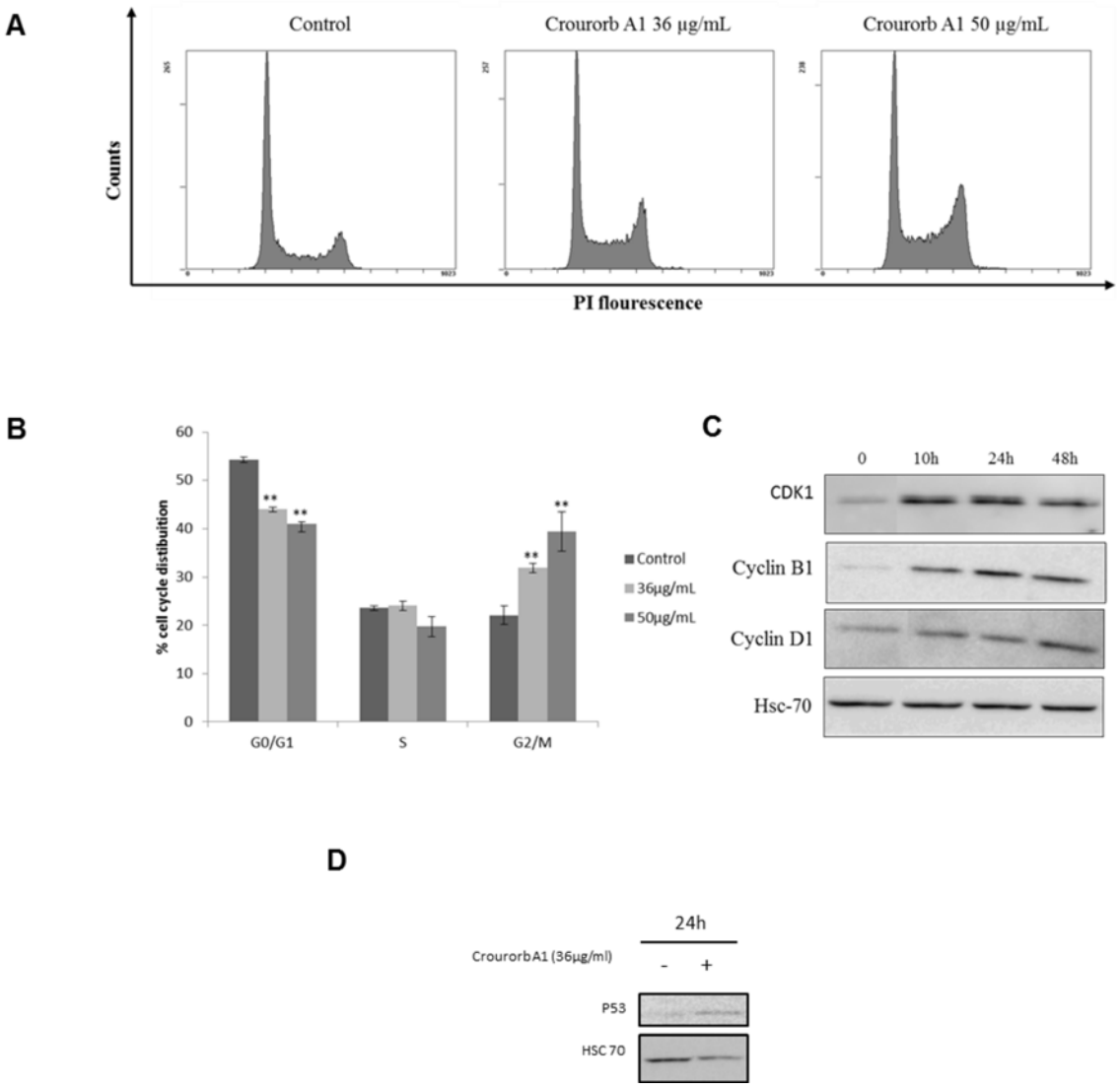

Figure 7

A

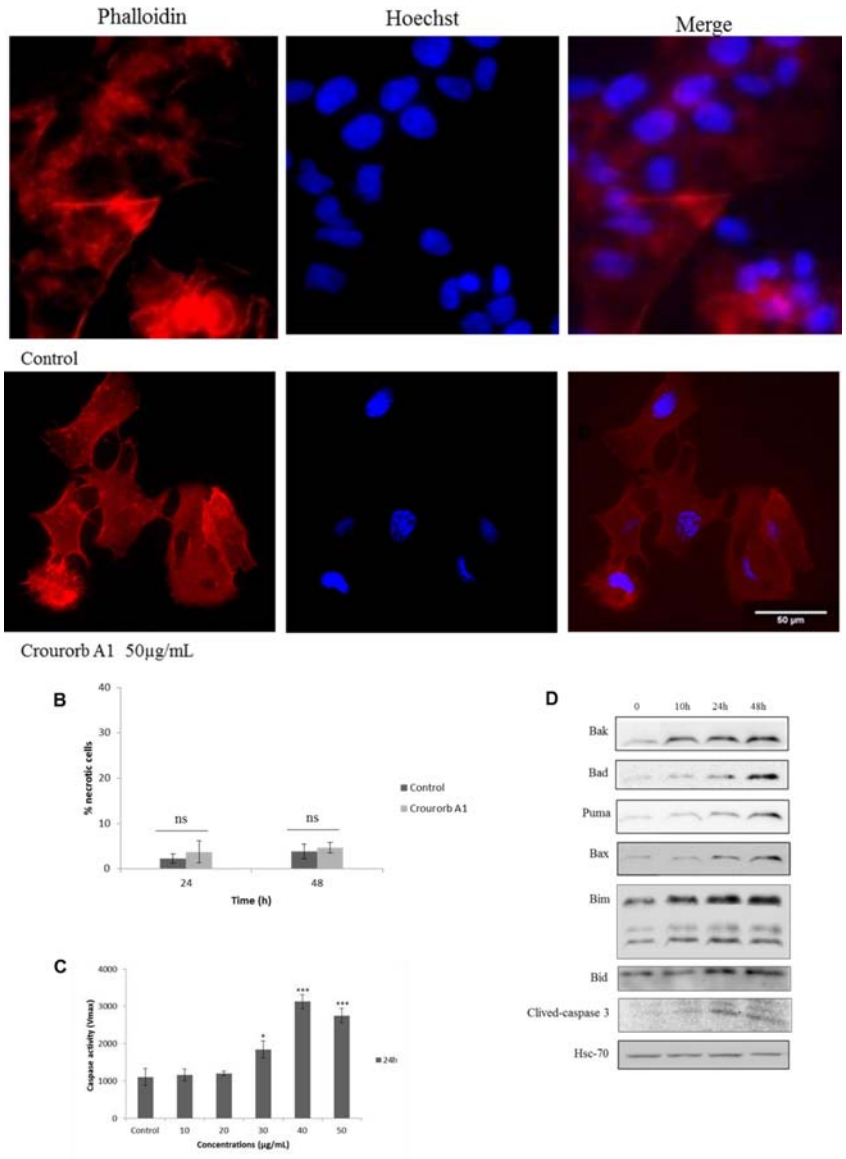

Figure 8

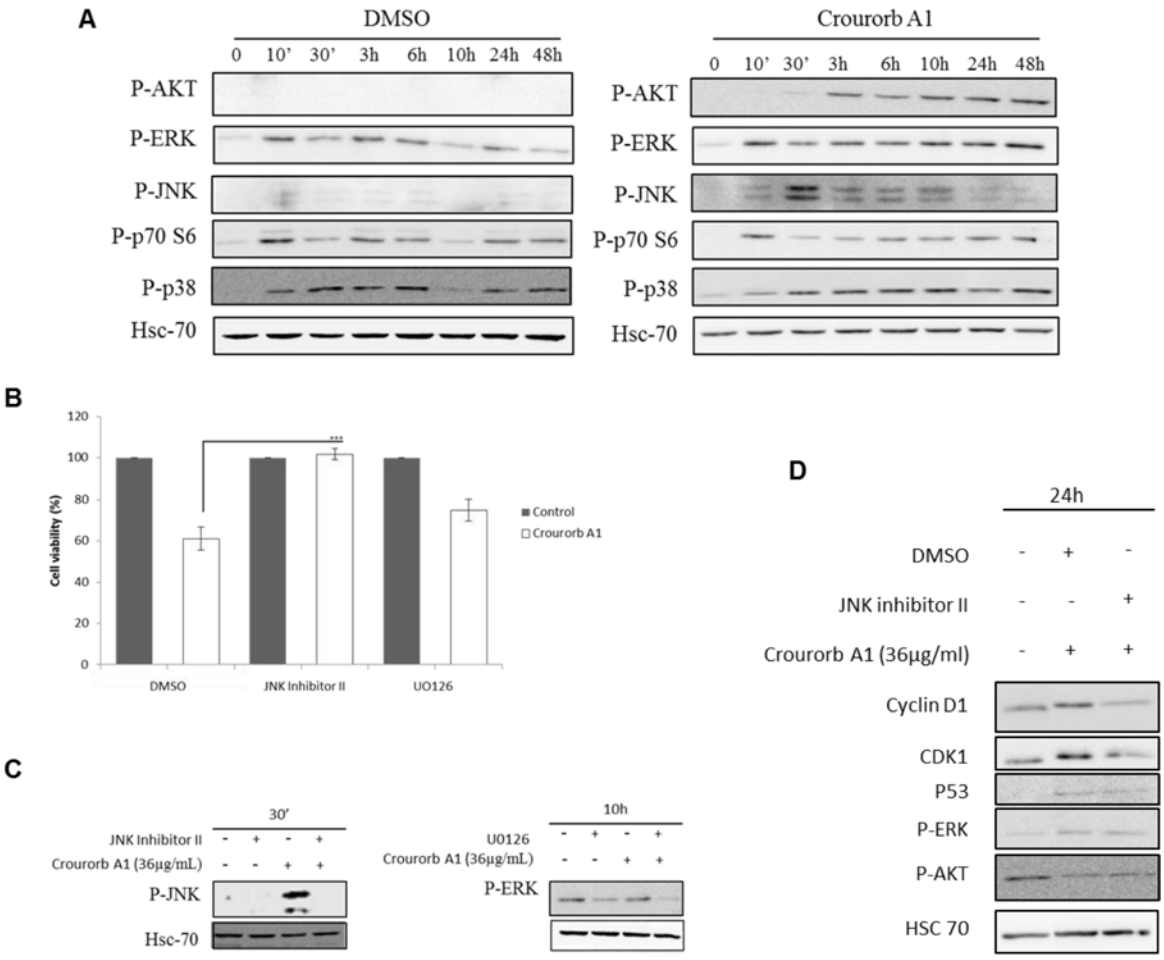

Figure 9

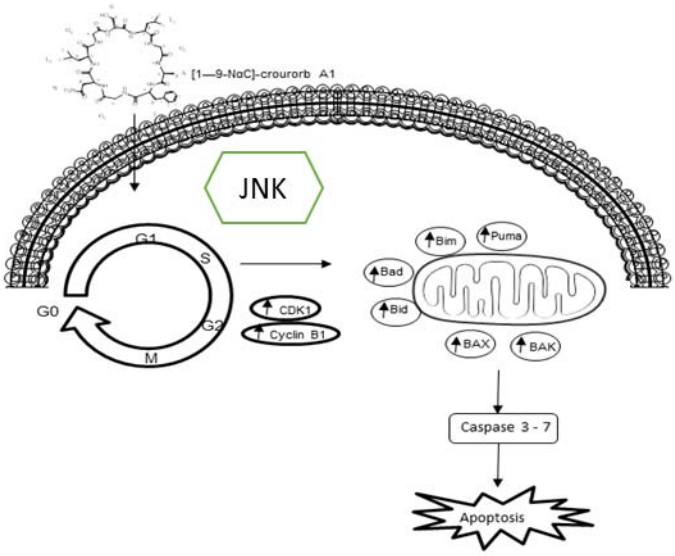

Tables

Table 1. IC_{50} values, given in µg/mL, for crourorb A1 on 2D Huh7 cell lines.

	IC_{50} (µg/mL)*±SD		
	24h	**48h**	**72h**
Crourorb A1	35.75±1.00	30.41±2.14	20.07±3.40
Cisplatin	23.19±0.21	4.26±1.44	2.26±0.24

*IC_{50} values were expressed as the concentration that inhibited the growth of cells by 50%. Results are expressed as the mean of three independent experiments±SD. Cisplatin was used as a positive control.

Table 2. IC_{50} values, given in μg/mL, for crourorb A1 on 3D Huh-7 cell lines.

Days of cultures	Collagen gel (mg/mL)	IC_{50} (μg/mL)±SD*	
		Crourorb A1	Cisplatin
6	0.75	62.10±4.70	42.50±6.30
	1.5	62.52±3.12	36.48±0.77

*IC_{50} values were expressed as the concentration that inhibited the growth of cells by 50%. Results are expressed as the mean of three independent experiments±SD. Cisplatin was used as a positive control.